High-mass X-ray Binaries: Illuminating the Passage from Massive Binaries to Merging Compact Objects
Proceedings IAU Symposium No. 346, 2019
L. M. Oskinova, E. Bozzo, T. Bulik & D. Gies, eds.

doi:10.1017/S1743921318007469

The black hole spin in coalescing binary black holes and high-mass X-ray binaries

Y. Qin[1,2], T. Fragos[1], G. Meynet[1], P. Marchant[2], V. Kalogera[2], J. Andrews[3,4], M. Sørensen[1] and H. F. Song[5,6]

[1]Geneva Observatory, University of Geneva, CH-1290 Sauverny, Switzerland
email: ying.qin@unige.ch

[2]Center for Interdisciplinary Exploration and Research in Astrophysics (CIERA) and Department of Physics and Astrophysics, Northwestern University, Evanston, IL 60208

[3]Foundation for Research and Technology - Hellas, IESL, Voutes, 71110 Heraklion, Greece

[4]Physics Department & Institute of Theoretical & Computational Physics, University of Crete, 71003 Heraklion, Crete, Greece

[5]College of Physics, Guizhou University, Guiyang City, Guizhou Province, 550025, P.R. China

[6]Key Laboratory for the Structure and Evolution of Celestial Objects, Chinese Academy of Sciences, Kunming 650011

Abstract. The six LIGO detections of merging black holes (BHs) allowed to infer slow spin values for the two pre-merging BHs. The three cases where the spins of the BHs can be determined in high-mass X-ray binaries (HMXBs) show that those BHs have high spin values. We discuss here scenarios explaining these differences in spin properties in these two classes of object.

Keywords. binaries: close binary stars; X-rays: binaries; black hole; gravitational waves

1. Introduction

Astrophysical BH can be fully described by its mass M and angular momentum $\vec{J}$. The dimensionless BH spin parameter a_* is defined as follows:

$$a_* = cJ/GM^2, \tag{1.1}$$

where c is the speed of light in vacuum and G is the gravitational constant. With the detection of the first gravitational wave event (Abbott *et al.* 2016a) by the Advanced Laser Interferometer Gravitational-Wave Observatory (AdLIGO) (LIGO Scientific Collaboration *et al.* 2015), the existence of the massive stellar BHs has been observationally demonstrated and a new window has been opened to directly study their properties. To date, AdLIGO has already detected six gravitational wave events and one high-significance event (Abbott *et al.* 2016a,b,c, 2017a,b,c), which are unambiguously believed to originate from the merger of binary BHs (BBHs).

Before the discovery of the GW events, X-ray binaries have been considered to be an ideal environment to indirectly measure BH's properties (McClintock 2006; McClintock, Narayan, & Steiner 2014; Reynolds 2014; Casares & Jonker 2014; Miller & Miller 2015). In low-mass X-ray binaries, the measured BH spins a_* cover the whole range (from 0 to 1) and this can be well explained via accretion from its companion after the BHs' formation (Fragos & McClintock 2015). However, for BHs in HMXBs, the currently measured spins are extremely high ($a_* > 0.8$). The donor star in a HMXB has a relatively short lifetime. Hence the BH can not accrete enough material to spin itself up. So the alternative possibility that such BHs were born with a high natal spin is preferred.

The Case-A mass transfer (MT) channel (MT is occurring when the BH progenitor is still on the MS.) was for the first time proposed by Valsecchi *et al.* (2010) to explaining the formation of M33 X-7. However, it was assumed that during the MS, solid body rotation implies necessarily that differential rotation is not considered. So this will not provide a trustable or quantitative prediction on the BH spin.

The paper is organized as follows. In §2, we introduce main methods used in the stellar and binary evolution models. The results of two BH spins in coalescing BBHs are shown in §3. We then present the main results of the BH spin in HMXBs §4. The main results are summarized in §5.

2. The main methods in the stellar and binary evolution models

To investigate BH spins in coalescing BBHs we use the Modules for Experiments in Stellar Astrophysics (MESA) code version 8118 (Paxton *et al.* 2011, 2013, 2015, 2018). The initial mass fraction of helium is given with a linearly increasing from Y = 0.2447 (Grevesse, Noels, & Sauval 1996) at Z = 0 to Y = 0.28 at Z = $Z_\odot$ (0.017 is taken as the solar metallicity $Z_\odot$ in Asplund, Grevesse, Sauval, & Scott 2009). The implementation of the stellar winds is clearly described in Marchant *et al.* (2016).

We model convection by using the standard mixing-length theory (Böhm-Vitense 1958) with a mixing-length parameter α_{ov} = 1.5 and apply the Schwarzschild criterion to treat the boundary of the convective zones, as well as a convective core overshooting parametrized with $\alpha_{ov} = 0.1$. The angular momentum transport and chemical mixing of material are treated as a diffusion process, which includes the Eddington-Sweet circulations, the Goldreich-Schubert-Fricke instability, and secular and dynamical shear mixing with an efficiency parameter $f_c = 1/30$ (Chaboyer & Zahn 1992).

Our work of the BH spin in HMXB is in preparation and the latest MESA version 10398 is used instead of version 8118. The tidal coefficient E_2 for computing the synchronization timescale of the tides is taken from Eq. 9 in Qin *et al.* (2018). Furthermore, the implementation of the tides is considered to only have an impact on the layers of outer readiative zones instead of all layers inside the star.

3. The BH spin in coalescing binary BHs

Since the first GW event was discovered, the proposed double BH formation channels can be divided into two main categories: the binary evolution channel and the dynamical formation channel. If the binary system evolves initially at a wide separation (i.e., several thousand solar radii), it will go through the "CE" phase that is still poorly understood ("CE" binary evolution channel, Phinney 1991; Tutukov & Yungelson 1993; Belczynski, Holz, Bulik, & O'Shaughnessy 2016; Tutukov & Cherepashchuk 2017; van den Heuvel, Portegies Zwart, & de Mink 2017; Inayoshi, Hirai, Kinugawa, & Hotokezaka 2017). Alternatively, if the two stars are in a close orbit and at low metallicity, both components will evolve chemically homogeneously (the CHE channel, de Mink & Mandel 2016; Marchant *et al.* 2016; Mandel & de Mink 2016; Song *et al.* 2016). In contrast, in the dynamical formation channel, the two BHs are born in different places of globular clusters and are brought together via dynamical friction.

Based on the "CE" binary evolution channel, the systematic studies on the two BHs' spins have been investigated in Qin *et al.* (2018). The progenitor of the first-born BH evolves initially like a single star, expands to a supergiant phase and then loses the hydrogen envelope via Roche-lobe overflow MT and wind mass loss. During this process, the star loses most of its angular momentum and forms a BH (first-born BH) with a negligible ($a_* \lesssim 0.1$) spin.

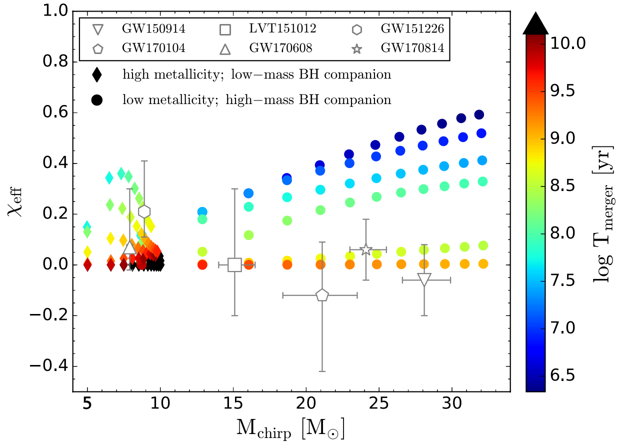

Figure 1. The time to merger ($T_{\rm merger}$) as a function of the $\chi_{\rm eff}$ and the $M_{\rm chirp}$. The colored dots correspond to a low metallicity (0.01 $Z_\odot$, $Z_\odot$ is the solar metallicity) grid, and the colored diamonds refer to a high metallicity ($Z_\odot$). Various empty symbols represent the currently observed events with corresponding error bars.

The post-CE system consists of a helium star and a BH with an orbital period of a few days. Such binary system was systematically investigated by taking into account different initial parameters, i.e., masses of two binary components, initial orbital period, initial rotation of the helium star, and its metallicity. It was found that the dimensionless spin a_* of the second-born BH covers the whole range (form 0 to 1). After the formation of the second-born BH, the merger timescale $T_{\rm merger}$ due to the GW emission can be derived (Peters 1964). In Fig. 1, we see that lower $\chi_{\rm eff}$ corresponds to a higher redshift. This is expected since to prevent the BH progenitors being accelerated by tides, the distance of the two binary components should be larger, hence a longer duration of the merger timescale $T_{\rm merger}$. In order to form lower values of $\chi_{\rm eff}$, their corresponding $T_{\rm merger}$ should be longer, which means such systems must have been formed at a higher redshift. This is consistent with the current observation from AdLIGO. However, we predict that with the improvement of AdLIGO's sensitivity in the future, the events with higher $\chi_{\rm eff}$ will be detected at a lower redshift. Furthermore, it is shown that more massive BHs (i.e. $\gtrsim$ 20 $M_\odot$) are not formed at a high redshit (i.e., solar metallicity). This is because the stars at a high metallicity loses more mass due to metallicity-dependent stellar winds and collapse to form less massive BHs.

Under the assumption of the direct core-collapse model, the BH progenitor directly forms a BH without any mass and angular momentum loss when it reaches the central carbon exhaustion.

4. The BH spin in high-mass X-ray binaries

A large fraction of all the massive binaries would go through the Case-A MT phase (Sana *et al.* 2012). The CHE is expected when the orbital period is shorter (shorter than about a few days) and the stars have a lower metallicity. Such a case was for the first time proposed by de Mink *et al.* (2009) in the binary evolution. In this part, we briefly introduce the main results on the study of BH HMXBs via the Case-A MT and the CHE channel. In Fig. 2, we show the detailed evolution processes of the BH progenitors' spins and orbital periods for the Case-A and the CHE. The binary system consisted of two stars (95.0 and 38.0 $M_\odot$ at 1/2 solar metallicity) goes through the Case-A MT channel when the initial orbital period is 3.25 days. The BH progenitor star speeds up during the MT phase, then decreases slowly and ends up with a fast-rotating BH at the end of

https://doi.org/10.1017/S1743921318007469 Published online by Cambridge University Press

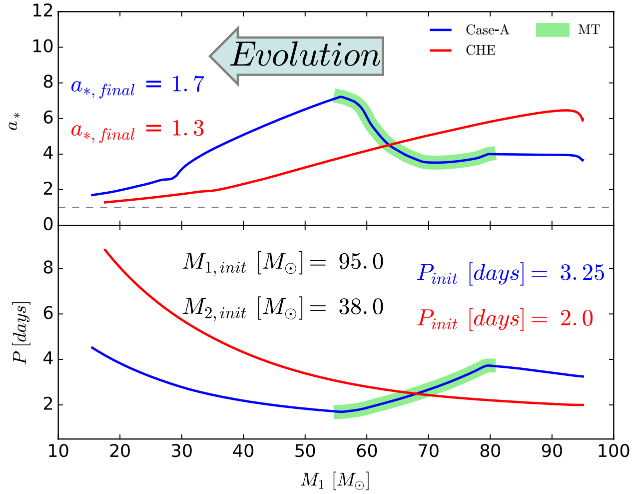

Figure 2. The spin of the resultant BH (upper panel) and orbital period (lower panel) as a function of the primary mass. Blue and red solid lines refer to the evolution of the Case-A MT and the CHE, respectively. The arrow "Evilution" represents the direction of each evolutional track and the MT phase is shown in green band. The horizontal dashed line represents the value of unity.

central carbon depletion. As shown in the lower panel of Fig. 2, the MT from the massive star (BH progenitor) onto its companion keeps the binary system tight. However, starting at the orbital period of 2.0 days, the system would go through the CHE instead of the Case-A MT channel. The BH progenitor continuously slows down and forms a BH with a_* around 1.0. Under this condition, the stellar winds mass-loss makes the orbit widening instead of shrinking. A fast-rotating BH for the two channels can be formed, while only shorter orbital period would be expected through the Case-A MT channel.

Here we highlight that the Tayler-Spruit dynamo (TS dynamo, Spruit 1999, 2002) plays a key role in forming a fast-rotating BH. For both channels, the BH progenitor keeps rotating fast during the MS. It does not evolve to a supergiant phase after the MS, but contracts after the helium surface abundance reaches a certain point. The angular momentum content of the BH progenitor will not be greatly changed during the period of this fast-shrinking phase. From this phase of fast shrinking, the evolution of the spin parameter is very different depending on the efficiency of the angular momentum transport mechanism. Only when a less efficient angular momentum transport mechanism than the one given by the TS dynamo is accounted for, a fast rotating BH is obtained. Otherwise, the BH will have a negligible spin. During that phase, tides are weak and thus have a small impact on the final spin of the BH.

We also created a big grid covering the initial parameter space of initial mass of the primary (from 20 - 100 $M_\odot$ with a step of 5 $M_\odot$), mass ratio q (from 0.25, 0.30, ..., 0.95) and orbital period (between 1 and 4 days with a step of 0.25 days, between 4 and 6 days with a step of 0.5 days). Here we only show a slice of our grid with mass ratio $q = 0.4$.

In Fig. 3, we present the best matches (blue track: M33 X-7, green track: Cygnus X-1 and red track: LMC X-1) with the current observations. Compared with the channel of the CHE, the Case-A MT channel results in a shorter orbit, which is consistent with current observations of the orbital periods. It is clearly shown in this figure, all the properties of LMC X-1 are well matched. For Cygnus X-1, the results are still acceptable and a better match will be expected with a higher resolution of the parameter space. In contrast, for M33 X-7, most the quantities are consistent with the observation, except

https://doi.org/10.1017/S1743921318007469 Published online by Cambridge University Press

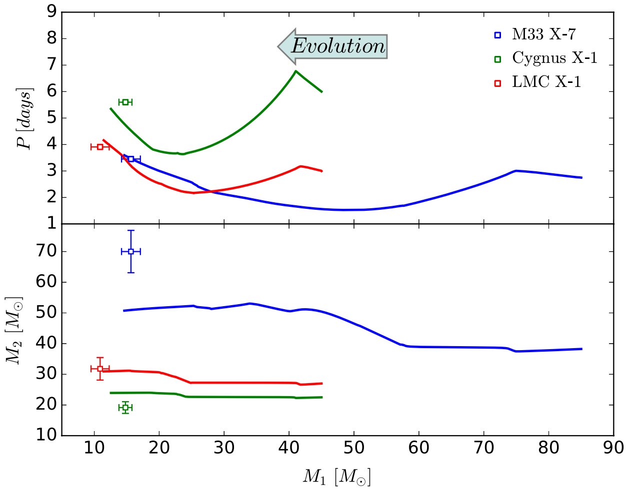

Figure 3. Orbital period (top panel) and secondary mass (bottom panel) as a function of primary mass. The properties of the observed systems are marked with blue, red and green squares for M33 X-7, Cygnus X-1 and LMC X-1, respectively. The arrow on the top panel shows the direction of the evolution.

the mass of the BH companion. This is because in our model, the companion star is being spun up due to the accreted material from the BH progenitor. When the companion star reaches its critical rotation, the MT becomes highly non-conservative. However, the MT efficiency is still uncertain. Had the MT been assumed to be conservative, as in Valsecchi *et al.* (2010), the mass of the BH companion could reach much higher values.

The nitrogen surface abundances of the BH companion stars between the Case-A MT and the CHE channel are significantly different. For the former channel, the mass is transferred from deep layers of the primary that have been reprocessed from the CNO cycle and hence this can largely enhance the nitrogen surface abundance of the secondary. In contrast, without the MT from the primary star of the CHE channel, no such high enhancement would be expected. Such results can be used for two purposes. First, the nitrogen surface abundance is a prediction that can be used to check the consistency of the models. Second, nitrogen surface abundance appears as a discriminating quantity, together with the orbital period, between the case-A MT and the CHE channel.

5. Conclusions

In this paper, we briefly describe our main results on the BH spin in two different BH binaries, namely, the coalescing BBHs and BH HMXBs. The BH in these two types of systems have very different BH spin measurements, which can be explained well by introducing different formation channels. For the "CE" binary evolution channel, the first-born BH has a negligible spin, while the second-born one covers the whole range of the spin (from 0 to 1). Besides, we expect the higher $\chi_{\rm eff}$ would be observed at lower redshits with the improvements of AdLIGO. On the other hand, with an assumption that the inefficient angular momentum transport is implemented after the MS of the BH progenitor, the currently observed BH spins in HMXBs can be well explained via the Case-A MT and the CHE channel. Compared to the CHE channel, the Case-A MT can form a HMXB in a tight orbit, which is consistent with the current observations. Hence The Case-A MT can be considered a potential channel to explain the current properties of Cygnus X-1, LMC X-1 and M33 X-7. Finally, we expect the nitrogen surface abundance

https://doi.org/10.1017/S1743921318007469 Published online by Cambridge University Press

of the BH companion star can be challenged from the observational point of view to distinguish the two channels.

Acknowledgements

This work was sponsored by the Chinese Scholarship Council (CSC). This project has received funding from the European Union's Horizon 2020 research and innovation programme under the Marie Sklodowska-Curie RISE action, grant agreement No 691164 (ASTROSTAT). TF is grateful for support from the SNSF Professorship grant (project number PP00P2_176868) the DNRF (Niels Bohr Professorship Program), the Carlsberg Foundation and the VILLUM FONDEN (project number 16599). The computations were performed at the University of Geneva on the Baobab computer cluster. All figures were made with the free Python module Matplotlib (Hunter 2007).

References

Abbott, B. P., Abbott, R., Abbott, T. D., *et al.* 2016, Physical Review Letters, 116, 061102
Abbott, B. P., Abbott, R., Abbott, T. D., *et al.* 2016, Physical Review Letters, 116, 241102
Abbott, B. P., Abbott, R., Abbott, T. D., *et al.* 2016, Physical Review X, 6, 041015
Abbott, B. P., Abbott, R., Abbott, T. D., *et al.* 2016, Physical Review Letters, 116, 241103
Abbott, B. P., Abbott, R., Abbott, T. D., *et al.* 2017, Physical Review Letters, 119, 161101
Abbott, B. P., Abbott, R., Abbott, T. D., *et al.* 2017, Physical Review Letters, 119, 141101
Abbott, B. P., Abbott, R., Abbott, T. D., *et al.* 2017, The Astrophysical Journal, 851, L35
Abbott, B. P., Abbott, R., Abbott, T. D., *et al.* 2017, Physical Review Letters, 118, 221101
Asplund, M., Grevesse, N., Sauval, A. J., & Scott, P. 2009, Annual Review of Astronomy and Astrophysics, 47, 481
Böhm-Vitense, E. 1958, Zeitschrift fur Astrophysik, 46, 108
Belczynski, K., Holz, D. E., Bulik, T., & O'Shaughnessy, R. 2016, Nature, 534, 512
Casares, J., & Jonker, P. G. 2014, Space Science Reviews, 183, 223
Chaboyer, B., & Zahn, J.-P. 1992, Astronomy and Astrophysics, 253, 173
de Mink, S. E., Cantiello, M., Langer, N., *et al.* 2009, Astronomy and Astrophysics, 497, 243
de Mink, S. E., & Mandel, I. 2016, Monthly Notices of the Royal Astronomical Society, 460, 3545
Fragos, T., & McClintock, J. E. 2015, The Astrophysical Journal, 800, 17
Grevesse, N., Noels, A., & Sauval, A. J. 1996, Cosmic Abundances, 99, 117
Hunter, J. D. 2007, Computing in Science and Engineering, 9, 90
Inayoshi, K., Hirai, R., Kinugawa, T., & Hotokezaka, K. 2017, Monthly Notices of the Royal Astronomical Society, 468, 5020
LIGO Scientific Collaboration, Aasi, J., Abbott, B. P., *et al.* 2015, Classical and Quantum Gravity, 32, 074001
Mandel, I., & de Mink, S. E. 2016, Monthly Notices of the Royal Astronomical Society, 458, 2634
Marchant, P., Langer, N., Podsiadlowski, P., Tauris, T. M., & Moriya, T. J. 2016, Astronomy and Astrophysics, 588, A50
McClintock, J. E. 2006, Bulletin of the American Astronomical Society, 38, 33.01
McClintock, J. E., Narayan, R., & Steiner, J. F. 2014, Space Science Reviews, 183, 295
Miller, M. C., & Miller, J. M. 2015, Physics Reports, 548, 1
Paxton, B., Bildsten, L., Dotter, A., *et al.* 2011, The Astrophysical Journal Supplement Series, 192, 3
Paxton, B., Cantiello, M., Arras, P., *et al.* 2013, The Astrophysical Journal Supplement Series, 208, 4
Paxton, B., Marchant, P., Schwab, J., *et al.* 2015, The Astrophysical Journal Supplement Series, 220, 15
Paxton, B., Schwab, J., Bauer, E. B., *et al.* 2018, The Astrophysical Journal Supplement Series, 234, 34

Peters, P. C. 1964, Physical Review, 136, 1224
Phinney, E. S. 1991, The Astrophysical Journal, 380, L17
Qin, Y., Fragos, T., Meynet, G., *et al.* 2018, Astronomy and Astrophysics, 616, A28
Remillard, R. A., & McClintock, J. E. 2006, Annual Review of Astronomy and Astrophysics, 44, 49
Reynolds, C. S. 2014, Space Science Reviews, 183, 277
Sana, H., de Mink, S. E., de Koter, A., *et al.* 2012, Science, 337, 444
Song, H. F., Meynet, G., Maeder, A., Ekström, S., & Eggenberger, P. 2016, Astronomy and Astrophysics, 585, A120
Spruit, H. C. 2002, Astronomy and Astrophysics, 381, 923
Spruit, H. C. 1999, Astronomy and Astrophysics, 349, 189
Tutukov, A. V., & Cherepashchuk, A. M. 2017, Astronomy Reports, 61, 833
Tutukov, A. V., & Yungelson, L. R. 1993, Monthly Notices of the Royal Astronomical Society, 260, 675
Valsecchi, F., Glebbeek, E., Farr, W. M., *et al.* 2010, Nature, 468, 77
van den Heuvel, E. P. J., Portegies Zwart, S. F., & de Mink, S. E. 2017, Monthly Notices of the Royal Astronomical Society, 471, 4256